

# Recovering Slices inside Translucent Media using Coaxial Multi-frequency Illumination

KENICHIRO TANAKA<sup>1,a)</sup> YASUHIRO MUKAIGAWA<sup>2</sup> YASUYUKI MATSUSHITA<sup>3</sup>  
YASUSHI YAGI<sup>1</sup>

## 1. Overview

Appearance of a translucent object is complex due to the composition of volumetric radiance emitted from all depths inside the object. In this paper, we propose a method for recovering radiance slices inside translucent objects, which are slices of volumetric radiance, using a coaxial projector-camera system. We use a depth-dependent point spread function (PSF) model and derive a relationship between the PSF and the frequency of projection patterns. By measuring the scene with varying projection pattern frequencies, we show that the radiance slices at certain depths can be linearly obtained by solving a system of equations that relate observed images, PSFs, and radiance slices. We show the effectiveness of the proposed method via real-world experiments.

## 2. Method

Observed intensity of a translucent object is the summation of volumetric radiances along the ray toward the observer. To achieve the goal of imaging radiance slices of a translucent object, we use the relationship between scene depths and the spatial spreads of their radiance represented by PSFs. The proposed method is built upon the high-frequency illumination based approach to separate direct and indirect light components [2], and we customize the original method for the radiance slice imaging by developing coaxial illumination and separation method.

### Depth-dependent PSF

The spread of radiance at a scene point inside a translucent object varies depending on its depth from the object surface due to scattering [3]. In general, the spatial spread of light can be expressed using PSFs. When we look at light rays emitted (or returned) from a specific depth in a translucent object, the PSF becomes sharper if the depth is shallower. On the other hand, it gently spreads if the depth gets deeper. In this manner, there is a close relationship between PSFs and depths, and we use this depth-dependent

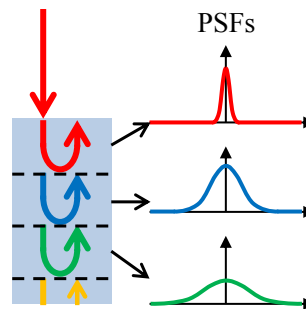


Fig. 1: Illustration of depth-dependent PSFs. Lights are spread depending on the depth.

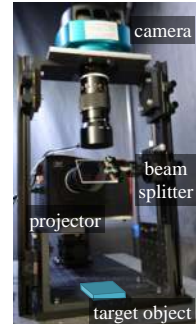


Fig. 2: Constructed coaxial measurement system. Coaxial setting can separate volumetric direct reflection.

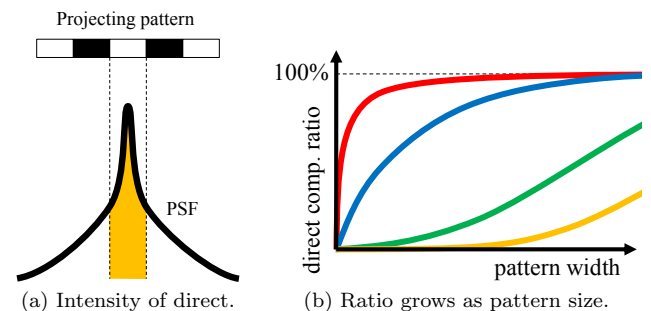


Fig. 3: Relationship between direct components and PSF. (a) The intensity of direct component can be approximate to the orange region of the PSF. This region is determined by the square size of projecting pattern. (b) The ratio of direct component grows as projected pattern size is larger. Moreover, the ratio grows faster as the PSF is sharper, while it grows slower as PSF is gentler.

PSF model for recovering radiance slices.

We assume that the PSFs are modeled by the radiative transfer equation (RTE) [1]. In the RTE model, observed intensity  $I$  is determined by the distance and observation angle. Using this term, the depth dependent PSF ( $h_d$ ) is expressed as

$$h_d(r) = I \left( \frac{d}{\cos \phi}, \phi \right), \phi = \tan^{-1} \frac{d}{r}. \quad (1)$$

Using this depth-dependent PSF, the observation ( $O$ ) is expressed by the convolution ( $\otimes$ ) between the actual depth radiance ( $C_d$ ) as

$$O = \sum_d C_d \otimes h_d. \quad (2)$$

<sup>1</sup> Osaka University

<sup>2</sup> Nara Institute of Science and Technology

<sup>3</sup> Microsoft Research Asia

<sup>a)</sup> tanaka@am.sanken.osaka-u.ac.jp

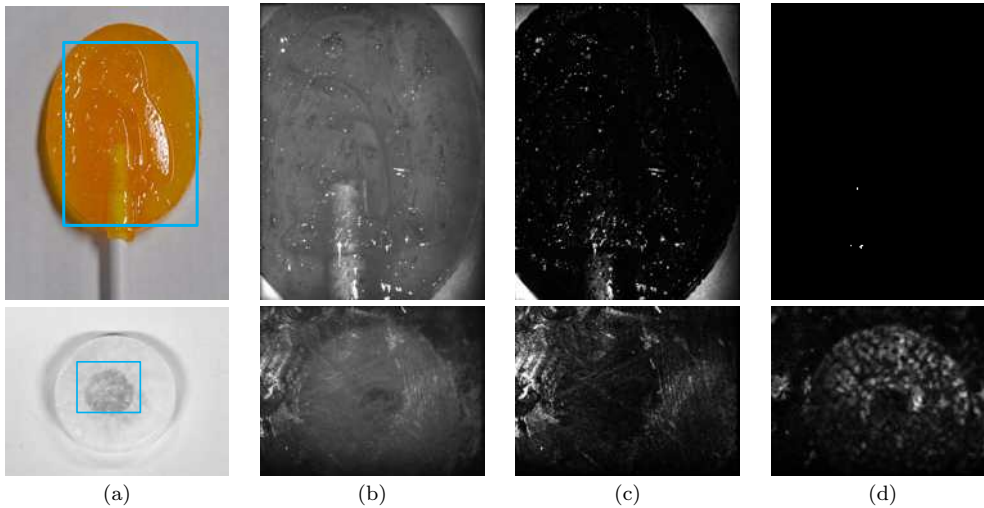


Fig. 4: Recovered radiance slices of a lollipop candy and wax object. (a) The target objects. We can see the stick in the candy (upper) and a coin inside the wax (lower). (b) Normal observation of the target objects indicated by blue rectangles. They contain all components of surface reflection, inside texture, and scattering. (c) component of  $d = 0$ . It is appeared that the glossy surface reflection of the candy and scratches on the surface of the wax. (d) component of  $d = 1$ . It is appeared that the stick of the candy and shape of the coin.

### Multi-frequency illumination

The original high-frequency illumination method [2] separates the direct ( $D_p$ ) and indirect ( $G_p$ ) components of light by projecting fine pitch ( $p$ ) checkered patterns:

$$O = D_p + G_p \quad (3)$$

Here, the ratio of direct components ( $r_d(p) = O/D_p$ ) is growing related to  $p$ , as shown in Fig. 3 (a). The growing curves as illustrated in Fig. 3 (b) vary depending on the shape of the PSFs.

The separated direct components  $D(p)$  by the high-frequency illumination with pattern size  $p$  can be expressed as a summation of radiances at each depth slice as

$$D(p) = \sum_d r_d(p) C_d, \quad (4)$$

where  $r_d(p)$  denotes the ratio of the direct component to the ordinary observation, which can be derived from the depth-dependent PSF  $h_d$ . Our method measures a set of direct component images  $D(p)$  by varying the pattern size  $p$  via multi-frequency illumination.

With the multi-frequency illumination under  $m$  frequencies of the patterns  $p(p_0, p_1, \dots, p_{m-1})$ , we can obtain a set of direct component images  $D(p)$ . Each of them can be expressed as an independent equation; thus Eq. (4) can be written by a matrix form as

$$\mathbf{d} = \mathbf{A}\mathbf{c}, \quad (5)$$

where

$$\mathbf{d} = \begin{bmatrix} D(p_0) & D(p_1) & \cdots & D(p_{m-1}) \end{bmatrix}^T$$

$$\mathbf{A} = \begin{bmatrix} r_{d_0}(p_0) & \cdots & r_{d_{n-1}}(p_0) \\ \vdots & \ddots & \vdots \\ r_{d_0}(p_{m-1}) & \cdots & r_{d_{n-1}}(p_{m-1}) \end{bmatrix}$$

$$\mathbf{c} = \begin{bmatrix} C_{d_0} & C_{d_1} & \cdots & C_{d_{n-1}} \end{bmatrix}^T.$$

Here,  $\mathbf{d}$  denotes a vector of direct components measured under  $m$  variations of the pattern sizes,  $\mathbf{c}$  denotes a vector of  $n$  layers of radiance slices, and  $\mathbf{A}$  denotes a matrix containing ratios of direct components computed from the projected pattern size and the depth-dependent PSF.

When the number of projected patterns is no smaller than the number of depth layers ( $m \geq n$ ) and the matrix  $A$  has rank( $n$ ), the radiance slices  $\mathbf{c}$  can be obtained in a least-squared sense by computing the pseudo-inverse  $\mathbf{A}^+$  as

$$\mathbf{c} = \mathbf{A}^+ \mathbf{d}. \quad (6)$$

### 3. Experiment

In this work, we develop a coaxial projector-camera system as shown in Fig. 2. Figure 4 is results of a lollipop candy and wax object. In these cases, We recover two radiance slices which contains informative texture. In the result of lollipop candy, there is glossy reflection on the surface ( $d = 0$  component). It is almost black because many lights are transmitted through the candy. On the other hand, the stick of a candy can be seen in the deeper slice. The lower row is a result of wax. There is a coin inside the wax and it can be seen as shown in normal photo. Texture of the surface such as scratches are appeared in the upper slice and the coin is appeared in the deeper slice.

### References

- [1] Narasimhan, S. and Nayar, S.: Shedding light on the weather, *Proceedings of the 2003 IEEE Computer Society Conference on Computer Vision and Pattern Recognition (CVPR)*, pp. 665–672 (2003).
- [2] Nayar, S. K., Krishnan, G., Grossberg, M. D. and Raskar, R.: Fast Separation of Direct and Global Components of a Scene using High Frequency Illumination, *Proceeding SIGGRAPH '06 ACM SIGGRAPH 2006 Papers*, pp. 935–944 (2006).
- [3] Shimizu, K., Tochio, K. and Kato, Y.: Improvement of translucent fluorescent images with a depth-dependent point-spread function, *Applied Optics*, Vol. 44, No. 11, pp. 2154–2161 (2005).